MedChemComm

Ligand-based homology modelling of the human CB2 receptor SR144528 antagonist binding site: a computational approach to explore the 1,5-diaryl pyrazole scaffold

Journal:	*MedChemComm*
Manuscript ID	MD-CAR-08-2015-000333.R1
Article Type:	Concise Article
Date Submitted by the Author:	09-Sep-2015
Complete List of Authors:	Cichero, Elena; University of Genoa, Department of Pharmacy; Elena Cichero, Menozzi, Giulia; University of genoa, Guariento, Sara; University of genoa, Fossa, Paola; University of genoa,

Ligand-based homology modelling of the human CB2 receptor SR144528 antagonist binding site: a computational approach to explore the 1,5-diaryl pyrazole scaffold

Elena Cichero, Giulia Menozzi, Sara Guariento and Paola Fossa*

Department of Pharmacy, University of Genoa, Viale Benedetto XV,3 - 16132 Genoa, Italy

* Corresponding author: phone: +39-010-3538238; fax: +39-010-3538358; e-mail:fossap@unige.it

Abstract

CB_1 and CB_2 receptors belong to the large family of G-protein coupled receptors (GPCRs), being involved in a wide variety of signal transduction. In this context, CB_2 selective compounds were described in literature to be active in different neuropathic and inflammatory pain models, showing also beneficial effects as neuroprotective agents. Indeed, CB_2 proved to be up-regulated in reactive microglial cells in Alzheimer's disease (AD) and Huntington's, suggesting a promising therapeutic panorama for CB_2 inverse agonist/antagonists. At present, the development of new selective CB2 antagonists is prevented by an unclear depiction of the reference antagonist SR144528 binding mode. Indeed, a few number of models concerning the CB2 receptor antagonist binding site have been proposed, leading sometimes to contradictory results. In this context, a specific *h*CB_2 ligand-based homology model in presence of the antagonist SR144528 was performed. Notably, the refined model also allowed us to explore the pyrazole scaffold as prototype for CB_2 ligand recognition and also to elucidate the CB1/CB2 structure-activity relationship of an in-house series of analogues we previously published. The derived information are expected to be a useful tool for guiding a much more focused and reliable CB_2 antagonists design.

Keywords: CB_2 antagonist, docking, homology modelling, 1,5-diarylpyrazoles, synthesis

Introduction

Cannabinoid receptors belong to the large family of G-protein coupled receptors (GPCRs) controlling a wide variety of signal transduction. They interact with cannabinoid drugs including the classical cannabinoids, such as Δ^9- tetrahydrocannabinol (Δ^9-THC), their synthetic analogues and the endogenous cannabinoids [1-4]. Currently, two subtypes of cannabinoid receptors have been cloned and pharmacologically characterized, the cannabinoid 1 receptor (CB_1) and the cannabinoid 2 receptor (CB_2), even if at present there is some experimental evidence supporting the existence of additional types of cannabinoid receptors [5-7]. CB_1 is mainly located within the central nervous system (CNS) at presynaptic nerve terminals, while CB_2 is mainly associated with immune system cells (they were identified in peripheral tissues, such as the spleen, tonsils and thymus). CB_2 selective compounds have been described in the literature to be active in different neuropathic and inflammatory pain models [8-12]. In addition, other studies also highlighted potentials roles for CB_2 in cancer [13, 14], multiple sclerosis [15] and bone regeneration [16,17]. Interestingly, CB_2 receptor has been recently found in CNS tissues showing some neuroprotective roles. Indeed, CB_2 proved to be up-regulated in reactive microglial cells in Alzheimer's disease (AD) and Huntington's, suggesting a promising therapeutic panorama for CB_2 inverse agonist/antagonists [18-20].

Moreover, CB_2 antagonists seem to possess an interesting profile concerning the inhibition of osteoclast formation and activity, in the treatment of obesity–associated inflammation, in insulin resistance and in non-alcoholic fatty liver disease [21]. Finally, more recent studies reported by Rizzo revealed a promising role played by CB_2 antagonists in reinforcing the antiepileptic action of WIN 55,212-2 [22].

Up to now only a limited number of CB_2 antagonist have been identified. 5-(4-chloro-3-methyl-phenyl)-1-(*p*-tolylmethyl)-N-(1,3,3-trimethylnorbornan-2-yl)pyrazole-3-carboxamide (SR144528) was the first one described in literature and therefore taken as reference compound for development of new analogues (Figure 1) [23].

Moreover Reggio et al. recently discussed a small series of new pyrazoles, structurally related to SR144528 (see **Ia** and **Ib**, Figure 1) [24]. Their work revealed the importance of the SR144528 amide function bearing a bulky hydrophobic group to explain its activity and also demonstrated that the substitution of the benzyl moiety with the phenyl one was allowed for CB_2 antagonism.

Notably, SR144528 shared the 1,5-disubstitued-pyrazole core displayed by the analogue SR141716A (Rimonabant), showing selective CB_2 and CB_1 antagonist activity, respectively.

On these basis, over the past decade we investigated a series of pyrazole derivatives closely related to the CB_1 antagonist SR141716A, with the aim at finding new cannabinoid receptor ligands (Figure 1) [25]. In particular, we focused our attention on a number of structural modifications displayed by switching a variable carboxamide function from the position 3 to the position 4 of the pyrazole core, and applying limited variations on the phenyl ring at position 5. On the contrary, the standard 2,4-dichlorophenyl ring at position 1 of SR141716A was maintained. Interestingly, all the derivatives conserved a modest cannabinoid receptor inhibitor activity, that increased with the presence of a *p*-I-phenyl ring at position 5 of the pyrazole core. In addition, a much more interesting affinity for the CB_1 or CB_2 was observed with a carboxamide group bearing a cyclopropyl ring or a cycloheptyl one, respectively.

Furthermore, more recent studies disclosed a number of selective CB2 ligands tuned substitutions onto the pyrazole positions 4 and 5 [26].

Together, all these results showed that a properly 1.5-disubtitued- pyrazole scaffold could display good electronic and steric features to be selectively anchored to the CB_1 or CB_2 recognition sites.

In tandem with the classical SAR-driven synthetic way, the rational drug design of new potential CB_1 or CB_2 ligands could be further addressed following a proper ligand-based (LB) and/or structure-based (SB) computational protocol [27,28]. Concerning this issue, during the last years we published a number of studies performed as LB and SB analyses of CB_1 antagonists and of several series of CB_2 agonists, without exploring the CB_2 antagonist activity [29-31].

In this context, up to now only a few number of SB molecular models of CB_2 receptor in complex with the antagonist compound was built and evaluated, leading sometimes to contradictory results [24,32,33].

Thus, in the present work, a model of the human CB_2 receptor (hCB$_2$) was developed by a LB homology modelling (LBHM), in order to carefully explore the pyrazole antagonist-CB_2 receptor interactions. The LBHM here presented was performed taking into account the antagonist SR144528 structural features and then evaluating the model reliability through a comparison with the mutagenesis data reported by Gouldson [34].

Successively, molecular docking studies were carried out on the aforementioned in-house series of previously synthesized pyrazoles and also on the most active compounds **I-III** (Figure 1), in order to evaluate the reliability of the built model and to reveal their putative binding mode toward CB_2 receptor. The final results are expected to be a useful tool to better point out any structural requirement or proper chemical substitution which could pave the way for identifying new potential CB_2 antagonists.

Results and Discussion

Ligand-based Homology modelling of the hCB$_2$ antagonist binding site

With the aim at gaining a better understanding of the human CB_2/**4** analogue interactions and also in order to derive useful information for the synthesis of new 1,5-diaryl-pyrazole derivatives as CB_2 antagonists, a specific ligand-based homology model of the human CB_2 receptor antagonist binding site was built. Thus, starting from our previously reported SB modelling studies about CB_2 receptor, we constructed a new refined model of hCB$_2$ using the LBHM approach, especially by taking into account the role of the pyrazole scaffold as preferred ligand. In details, the LBHM here applied should be considered as an evolution of the conventional homology modelling (HM), based on the same assumptions discussed by Moro et al. concerning the adenosine receptor LBHM case study [35] . This computational option is very useful when one wishes to build a homology model in the

presence of a ligand docked into the primary template and was widely and fruitfully used by us to build GPCR as well as various enzyme models [36-38].

In particular, we started our work from the standard HM approach we previously described, followed by molecular dynamics simulations (MD), that allowed us to derive a *h*CB_2 receptor model in complex with the agonist compound WIN-55,212-2. Briefly, the derived model displayed a CB_2 agonist recognition site which proved to be delimited by TM3, TM5 and TM6, being in agreement with site-directed mutagenesis data [27].

Successively, the same model was used as template to simulate the CB_2 LBHM (in presence of the pyrazole SR144528), that is here presented. The model was expected to be built up by taking into account any conformational change induced by the pyrazole ligand, as shown in the schematic representation of the LBHM protocol in Figure 2.

Notably, the putative agonist binding site of the standard *h*CB_2 model derived in the previous work corresponded with the most probable recognition cavity identified by the MOE Site finder module. On the contrary, the potential region prone to be involved in the antagonist contacts, which was hypothesized on the basis of mutagenesis data, fell in the lower scored sites.

In the specific case of the LBHM here reported, any steric and electrostatic variation induced by the SR144528 chemical structure during the model building, led to a final LBHM model whose shape and volume resulted highly modulated. Indeed, the molecular volume of the best scored binding site, changed from the 1490$Å^3$ of the standard HM-MD driven model agonist binding site, to the 1813$Å^3$ of the LBHM-driven one (corresponding to the antagonist binding site), without altering the overall receptor topology (Fig. 3).

The most probable interaction site of LBHM-driven model, as identified by the MOE Site finder module, included most of the reported residues involved in the antagonist binding (see mutagenesis data) [32]. The binding cavity reorganization induced by ligand interaction was caused by quite a conformational change of a number of amino acid side chains, belonging to TM3, TM4 and TM5 (Volume = 1813 $Å^3$). More in details, the antagonist SR144528 binding site included the following

residues: (*i*) L107, I110, G111, T114, M115 and T118 in TM3; (*ii*) L160, S161, L163, V164, S165, P168, L169 in TM4 and (*iii*) Y190, L191, W194, L195, F197, I198, F202 in TM5. Notably, our results were in agreement with those discussed by Montero et al. about the putative CB_2 binding site [39].

Taking into account the SR144528 refined docking solution, it can be observed that the nitrogen atom at the position 2 of the pyrazole moiety displayed one H-bond interaction with the T118 and S165 side chains, while the carbonyl oxygen showed one H-bond with the S165 side chain and a weaker one with S161 (Fig. 4). The 4-chloro,3-methyl-phenyl at the position 5 of the pyrazole ring established Van der Waals interactions and π–π stacking with L167, L195 and Y190, W194 respectively. The benzyl group at the position 1 of the pyrazole moiety was oriented towards the hydrophobic CB_2 cavity including residues I110, P168 and L169. On the other hand, the norbornane portion was oriented towards L160, V164, F197 and F202.

The reliability of the obtained LBHM *h*CB_2 model was verified comparing the key pattern of recognition here identified with those disclosed through mutagenesis data experiments. Indeed, Gouldson highlighted that SR144528 at 10^{-6} M failed to compete with [3H]WIN 55212-2 for binding to the S161A and S165A mutated CB_2 receptors [34].

On these positive results, the LBHM was therefore evaluated as a suitable structure-based tool to be used for rational drug design process. Accordingly, the model allowed us to carefully investigate the classical SAR of the in-house previously synthesized pyrazoles (**4a-4i**; Table 1) so as of **I-III**, through automated docking simulations (Table 2).

Automated molecular docking of I-III

In this work we explored the reliability of the derived LBHM running docking analyses of the potent SR144528-related compounds **Ia**, **Ib**, **II** and **III**.

According to our calculation, all of them shared a quite similar behaviour if compared with the reference pyrazole, especially detecting the same aforementioned hydrophobic contacts through the portion linked to the carboxamide group and the substituents onto the pyrazole core.

Therefore, any difference we observed revolved around the pattern of H-bonds involving the carbonyl group and the N1 nitrogen atom.

Interestingly, docking results concerning **Ia** gave an interesting explanation of the slightly switched docking mode of the SR144528 analogues, being chemically different from SR144528 only for a phenyl ring (instead of a benzyl one) linked to the pyrazole position 1.

Indeed, in absence of a flexible benzyl moiety onto the N1 nitrogen atom, **Ia** moved to interact with the upper region of the TM crevice, with respect to the reference compound. As a consequence, the **Ia** carbonyl function and the N2 nitrogen atom were involved in H-bonds with S165 and T114, respectively (Figure 5).

Moreover, the **Ib** analogue (bearing the benzyl substituent in N1) was able to display one H-bond between N2 and S165, while the carbonyl oxygen showed one H-bond with T118.

The most potent compound **II** was characterized by H-bonds between the carbonyl oxygen atom and S161 and S165, while the N2 atom interacted with T114 (Figure 6). Notably, the pyrrole ring at the pyrazole position 5 was able to play the same role of the SR144528 di-substituted phenyl ring, interacting by Van der Waals contacts and π–π stacking with L167, L195 and Y190.

Conversely, **III** showed a different docking mode, being the only one among **I**-**III** to display a *trans* conformation around the dihedral angle delimited by the carbonyl group and the pyrazole N2 and C3 atoms (Figure 7). This kind of behaviour could be due to the much more bulky and flexible group (benzyl moiety) linked to the carboxamide function, causing an overturned disposition within the binding site. Therefore, the oxygen atom was H-bonded to T114 and S165, while N2 was oriented towards the opposite side. Accordingly, **III** is less potent than the corresponding congener **II**.

Taking into account all these data, it should be noticed that for an high CB2 affinity level, a *cis* conformation within the aforementioned dihedral angle is preferred, opening the possibility of interact with the key residues S161, S165, T114 and T118. For the *trans* one, the presence of rigid groups at the pyrazole positions 1 and 5 becomes mandatory. Indeed, this kind of substituent moves the ligand to the upper region of the TM crevice and also allows any interaction with T114.

Automated molecular docking of the in-house pyrazoles 4a-4i

With the aim at derive new insights for the development of new pyrazoles, the main issues to be addressed were to clarify the role played by the shifted carboxamide and the linked R_1 substituents and the effect caused by a rigid group connected to the N1 nitrogen atom of **4a-4i**.

On the basis of our calculations, all of them proved to partially mimic the SR144528 binding mode, suggesting that our compounds could reasonably act as CB_2 antagonists.

In details, the compounds carboxamide nitrogen and oxygen atoms were quite aligned with the reference compound nitrogen atom and with the methylene of the benzyl group, respectively. Accordingly, the most interesting derivatives **4b**, **4e**, **4g**, **4i** proved to display one H-bond between the amide nitrogen atom and the side-chain of key residue S165, as previously described for SR144528 (Fig. 8).

In addition, **4e** bearing a hindered R_1 group, proved to properly occupy the receptor region delimited by L160, V164, F197 and F202, as underlined for the SR144528 norbornane cycle (Fig. 9).

Interestingly, this compound was much more potent as CB_2 rather than CB_1 ligands. Concerning this issue, it should be observed that the CB_2 V164 corresponds to an isoleucine residue at the corresponding position of the CB_1 receptor, underlying a precise steric limitation to be guaranteed for CB_1-ligand recognition, which turns in CB_2 antagonist selectivity [39].

On the other hand, the phenyl ring at the pyrazole position 5 showed the same interactions detected by the SR144528 benzyl as well as the pyrazole core and the R_3 substituent were able to mimic the

SR144528 phenyl groups. Interestingly, the presence of a bulky group on the R_2 *para* position proved to be beneficial, being the phenyl ring located in a deep receptor cavity including I110, T114, L169 and L182.

Therefore, **4a-4i** displayed a number of Van der Waals contacts between R_1 portion and L160, V164 and W194 side-chains, and π–π stacking between the two R_2 and R_3 phenyl ring and Y190. In addition, both the two aromatic cores were engaged in hydrophobic contacts with I110, L169, L182, L191 and L195.

Notably, in absence of a flexible benzyl moiety onto the N1 nitrogen atom, the compounds were anchored much more to the upper region of the TM crevice (if compared with SR144528) as we previously discussed about the most potent **Ia**, **II** and **III**. Consequently, the compound **4** R_1 portion was frequently unable to guarantee a further stabilizing H-bond with S165, that instead was shown by the SR144528 carbonyl group.

In addition, the selected poses highlighted a preferred *trans* conformation within the dihedral angle delimited by the carbonyl group and the pyrazole C4 and C5 atoms, in any case properly moving the carboxamide function towards V164 and F197. Notably, this kind of conformation together with the presence of the crucial amide group switched from the position 3 to the position 4 of the pyrazole core, oriented only the carboxamide nitrogen atom near the key residue S165, being the oxygen projected toward the opposite side. Nevertheless, this ligand conformation displayed N2 in proximity of T114, suggesting that an interaction with this residue should be tuned through further optimized substituents at the pyrazole positions 1 and 5.

Experimental

Data set

SR144528, **I-III** and the in-house compounds (Table 1) were built, parameterized (Gasteiger-Huckel method) and energy minimized within MOE using MMFF94 forcefield [40].

Ligand-Based Human CB_2 Receptor Homology Modeling

In this work, we constructed a new refined model of *h*CB_2 receptor using the LBHM approach. Briefly, the ligand-based homology modeling is performed by the proper handling of insertions and deletions of any selected extra-atoms during the energy tests and minimization stages of the modelling procedure. This computational option is very useful when one wishes to build a homology model in the presence of a ligand docked into the primary template. In particular, we focused our attention on the role of the SR144528 pyrazole scaffold, taken as preferred ligand.

Therefore, we started our work from the standard HM approach we recently described, followed by molecular dynamics simulations (MD), that allowed us to derive a *h*CB_2 receptor model in complex with the agonist compound WIN-55,212-2 [27]. Briefly, the previously built *h*CB_2 model was generated starting from the X ray structures of human β_2 adrenoreceptor (PDB code: 2RH1), A2A adenosine receptor (PDB code: 3EML) and rhodopsin bovine (PDB: 1F88) as GPCR templates. Then, the derived model was refined through docking analysis and MD performed on the agonist compound WIN-55,212-2. Following this procedure, the CB_2 agonist recognition site was investigated, proving to be delimited by TM3, TM5 and TM6. Successively, the same model was used as template to simulate the CB_2 LBHM, in presence of the pyrazole SR144528, docked in the area around (5Å distance) the key residue S165, as highlighted by mutagenesis experiments [34].

Thus, the protein structure was built and minimized with MOE [39] using the AMBER94 force field [41]. The minimizations were carried out by the 1000 steps of steepest descent followed by conjugate gradient minimization until the rms gradient of the potential energy was less than 0.1 kcal mol^{-1} $Å^{-1}$. The derived CB_2 LBHM was refined through a rotamer exploration of all side chains

involved in the antagonist-binding cavity, by rotamer explorer module of MOE. The obtained model backbone conformation was evaluated by inspection of Ramachandran plot, chi plot and clash contacts reports, showing absence of outliers. Finally, the protein-SR144528 complex stability was successfully assessed using a short ~1 ps run of molecular dynamics (MD) at constant temperature, followed by an all-atom energy minimization (LowModeMD implemented in MOE software).

Molecular docking of CB_2 agonists

In order to develop a LBHM of the *h*CB_2 receptor, the antagonist SR144528 was docked into the CB_2 model previously built using the MOE-DOCK tool. The compound best-docked pose, evaluated in terms of "London dG", was refined by energy minimization (MMFF94) and rescored according to "Affinity dG" (kcal/mol of total estimated binding energy) and also following H-bond preference criteria.

On the basis of the obtained *h*CB_2/ SR144528 LBHM, the in-house compounds **4** binding mode were explore by means of MOE-DOCK tool. Then, the best docking geometry (selected on the basis of the scoring functions) was refined by ligand/protein complex energy minimization (CHARMM27) by means of the MOE software. Finally, the protein-pyrazole complex stability was successfully assessed using a short ~1 ps run of molecular dynamics (MD) at constant temperature, followed by an all-atom energy minimization (LowModeMD implemented in MOE software). This kind of module allowed to perform an exhaustive conformational analysis of the ligand-receptor binding site complex, as we already discussed about other case studies, where it proved to be useful for a preliminary evaluation of docking poses [42].

Conclusions

The present work deals with the development of a ligand-based homology model of the human CB_2 receptor, which allowed us to carefully analyse the putative binding mode of the reference compound SR144528. The agreement with mutagenesis data proved that the LBHM we discussed

may be a reliable tool to be used in the process of CB_2 antagonists design. As a further LBHM evaluation, the following docking study of a series of in-house pyrazole developed as CB_2 ligands so as of a number of potent compounds described in literature (**I**-**III**) allowed to point out a number of key features involved in CB_2 recognition. In particular, the role played by the carboxamide function and of the substituent linked to the pyrazole position 1 were investigated and discussed.

On all these basis, it was expected that SR144528 analogues including 3-carboxamide substituted derivatives bearing a rigid and bulky group linked to the amide function, in tandem with proper decoration onto to aromatic rings at the position 1 and 5, could represent promising scaffolds to be developed as selective CB_2 antagonists. In addition, also 4-carboxamide substituted pyrazoles should be optimized with inverted amides connecting the pyrazole position 4 and an hydrophobic group linked to the carbonyl portion of the newly compounds.

Accordingly, the pyrazole scaffold still appears as a promising and challenging opportunity for the development of new CB_2 ligands.

Acknowledgements

This work was financially supported by the University of Genoa. Authors would like to Mr. V. Ruocco for the informatics support to calculations.

Conflict of Interest The authors declare that they have no conflict of interest.

References

1. S.L. Palmer, G.A. Thakur, A. Makriyannis *Chem. Phys. Lipids,* 2002*,* **121**, 3-19.

2. J.L. Wiley, B.R. Martin *Chem Phys Lipids*, 2002, **121**, 57-63.

3. R.G. Pertwee *Neurobiol.,* 2001, **63**, 569-611.

4. P. Goya, N. Jagerovic, L. Hernandez-Folgado, M.I. Martin, *Mini Rev. Med. Chem.*, 2003, **3**, 765-772.

5. A. Calignano, G. La Rana, D. Piomelli *Eur. J. Pharmacol.*, 2001, **419**, 191-198.

6. V. Di Marzo, C.S. Breivogel, Q. Tao, D.T. Bridgen, R.K. Razdan, A.M. Zimmer, A. Zimmer, B.R. Martin BR *Neurochemistry*, 2000, **75**, 2434-2444.

7. N. Hájos, C. Ledent, T.F. Freund Neuroscience, 2000, **12**, 3239-3249.

8. G.T. Whiteside, G.P. Lee, K.J. Valenzano *Curr. Med. Chem.*, 2007, **14**, 917 -936.

9. C. Turcotte, F. Chouinard, J.S. Lefebvre, N. Flamand, *J. Leukoc. Biol.*, 2015, **97**, 1049-1070.

10. W.L. Mitchell, G.M.P. Giblin, A. Naylor, A.J. Eatherton, B.P. Slingsby, D.A. Rawlings, K.S. Jandu, C.P. Haslam, A.J. Brown, P. Goldsmith, N.M. Clayton, A.W. Wilson, I.P. Chessell, R.H. Green, A.R. Whittington, I.D. Wall *Bioorg Med Chem Lett*., 2009, **19**, 259-263.

11. J. Guindon, A.G. Hohmann *Br. J. Pharmacol*., 2008, **153**:319-334.

12. A.D. Khanolkar, D. Lu, M. Ibrahim, R.I. Duclos, G.A. Thakur, T.P. Malan, F. Porreca, V. Veerappan, X. Tian, C. George, D.A. Parrish, D.P. Papahatjis, A J. Makriyannis *J Med. Chem.*, 2007, **50**, 6493-6500

13. S. Sarfaraz, F. Afaq, V.M. Adhami, H. Mukhtar *Cancer Res.*, 2005, **65**, 1635–1641.

14. R.J. McKallip, W. Jia, J. Schlomer, J.W. Warren, P.S. Nagarkatti, M. Nagarkatti *Molecular Pharmacology*, 2006, **70**, 897-908.

15. R.G. Pertwee Pharmocol. Therapeut., 2002, **95**, 165-174.

16. O. Ofek, M. Karsak, N. Leclerc, M. Fogel, B. Frenkel, K. Wright, J. Tam, M. Attar-Namdar, V. Kram, E. Shohami, R. Mechoulam, A. Zimmer, I. Bab *Proc. Natl. Acad. Sci. U.S.A*., 2006, **103**, 696-701.

17. A.I. Idris, R.J. Van't Hof, I.R. Greig, S.A. Ridge, D. Baker, R.A. Ross, S.H. Ralston .*Nat. Med*., 2005, **11**, 774-779.

18. J. Fernandez-Ruiz, J. Romero, G. Velasco, R.M. Tolon, J.A. Ramos, M. Guzman *Trends Pharmacol. Sci.*, 2007, **28**, 39-45.

19. M. Maccarrone, N. Battista, D. Centonze, D. *Prog. Neurobiol*., 2007, **81**, 349-379.

20. D. Centonze, A. Finazzi-Agro, G. Bernardi, M. Maccarrone *Trends Pharmacol Sci*., 2007, **28**, 180-187.

21. V. Deveaux, T. Cadoudal, Y. Ichigotani, F. Teixeira-Clerc, A. Louvet, S. Manin, J. Tran-Van Nhieu, M.P. Belot, A. Zimmer, P. Even, P.D. Cani, C. Knauf, R. Burcelin, A. Bertola, Y. Le Marchand-Bruste, P. Gual, A. Mallat, S. Lotersztajn *PLoS One*, 2009, **6** e5844

22. V. Rizzo, F. Carletti, G. Gambini, G. Schiera, C. Cannizzaro, G. Ferraro, P. Sardo *Epilepsy Research*, 2014, **108**, 1711-1718.

23. M. Rinaldi-Carmona, F. Barth, J. Millan, J.M. Derocq, P. Casellas, C. Congy, D. Oustric, M. Sarran, M. Bouaboula, B. Calandra, M. Portier, D. Shire, J.C. Brelière, G.L. Le Fur *J Pharmacol Exp Ther.*, 1998, **284**, 644-650

24. E. Kotsikorou, F. Navas 3rd; M.J. Roche, A.F. Gilliam, B.F. Thomas, H.H. Seltzman, P. Kumar, Z.H. Song, D.P. Hurst, D.L. Lynch, P.H. Reggio *J. Med. Chem.*, 2013, **56**, 6593-6612.

25. G. Menozzi, P. Fossa, E. Cichero, A. Spallarossa, A. Ranise, L. Mosti *Eur. J. Med. Chem*., 2008, **43**, 2627-2638.

26. F. Piscitelli, A. Ligresti, G. La Regina, V. Gatti, A. Brizzi, S. Pasquini , M. Allarà, M.A.M. Carai, E. Novellino, G. Colombo, V. Di Marzo, F. Corelli, R. Silvestri *Eur. J. Med. Chem.*, 2011, **46**, 5641-5653.

27. E. Cichero, A. Ligresti, M. Allarà, V. di Marzo, Z. Lazzati, P. D'Ursi, A. Marabotti, L. Milanesi, A. Spallarossa, A. Ranise, P. Fossa *Eur. J. Med. Chem.*, 2011, **46**, 4489-4505.

28.. E.R. Hickey, R. Zindell, P.F. Cirillo, L. Wu, M. Ermann, A.K. Berry, D.S. Thomson, C. Albrecht, M.J. Gemkow, D. Riether *Bioorg. Med. Chem. Lett.*, 2015, **25**, 575-580.

29. E. Cichero, G. Menozzi, A. Spallarossa, L. Mosti, P. Fossa *J. Mol. Model.*, 2008, **14**, 1131-1145.

30. E. Cichero, S. Cesarini, L. Mosti, P. Fossa *J. Mol. Model*., 2010, **16**, 677-691.

31. E. Cichero, S. Cesarini, L. Mosti, P. Fossa *J. Mol. Model*., 2010, **16**, 1481-1498.

32. S. Bertini, T. Parkkari, J.R. Savinainen, C. Arena, G. Saccomanni, S. Saguto, A. Ligresti, M. Allarà, A. Bruno, L. Marinelli, V. Di Marzo, E. Novellino, C. Manera, M. Macchia *Eur J Med Chem.*, 2015, **27**, 526-536.

33. J. El Bakali, G.G. Muccioli, N. Renault, D. Pradal, M. Body-Malapel, M. Djouina, L. Hamtiaux, V. Andrzejak, P. Desreumaux, P. Chavatte, D.M. Lambert, R. Millet *J Med. Chem.*, 2010, **53**, 7918-7931.

34. P. Gouldson, B. Calandra, P. Legoux, A. Kernéis, M. Rinaldi-Carmona, F. Barth, G. Le Fur, P. Ferrara, D. Shire *Eur. J. Pharmacol*., 2000, **28**, 17-25.

35. S. Moro, F. Deflorian, M. Bacilieri, G. Spalluto *Curr. Pharm. Des*., 2006, **12**, 2175-2185.

36. E. Cichero, S. Espinoza, R.R. Gainetdinov, L. Brasili, P. Fossa *Chem. Biol. Drug. Des*., 2013, **81**, 509-516.

37. E. Cichero, S. Espinoza, S. Franchini, S. Guariento, L. Brasili, R.R. Gainetdinov, P. Fossa *Chem. Biol. Drug. Des*., 2014, **84**, 712-720.

38. E. Cichero E, P. D'Ursi, M. Moscatelli, O. Bruno, A. Orro, C. Rotolo, L. Milanesi, P. Fossa *Chem. Biol. Drug. Des.*, 2013, **82**, 718-731.

39. C. Montero, N.E. Campillo, P. Goya, J.A. Páez *Eur. J. Med. Chem*., 2005, **40**, 75-83.

40. MOE: Chemical Computing Group Inc . Montreal. H3A 2R7 Canada. http://www.chemcomp.com

41. F.A. Momany, J.L. Willet *Carbohydr Res*., 2000, **326**, 194-209.

42. P. Fossa, E. Cichero, *Bioorg. Med. Chem*., 2015, **23**, 3215-3220.

Table 1: Chemical structure and cannabinoid receptor binding affinity of previously synthesized compounds **4a-4i**

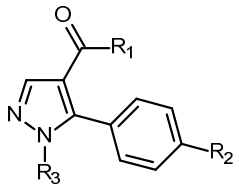

Compound	R_1	R_2	R_3	Displacement [%] hCB$_1$ receptor[a]	Displacement [%] hCB$_2$ receptor[b]
4a	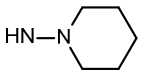	Cl	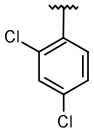	79	37
4b	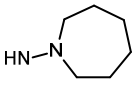	Cl	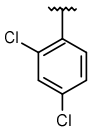	75	64
4c	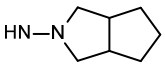	Cl	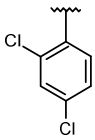	86	56
4d	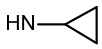	Cl	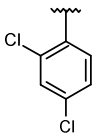	87 (K_i = 0.85 ± 0.03 μM)	30 (K_i = 21 ± 0.6 μM)
4e	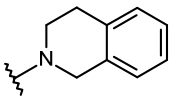	Cl	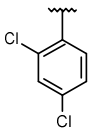	58	69
4f	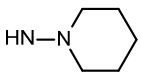	Br	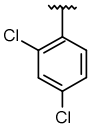	74	55
4g	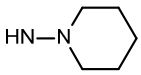	I	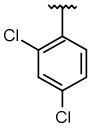	94 (K_i = 1.3 ± 0.05 μM)	84 (K_i = 1.9 ± 0.06 μM)
4h	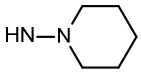	-CH_3	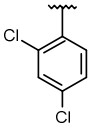	29	27
4i	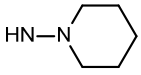	-OCH_3	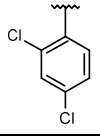	58	70

[a] Data reported as percent (n = 2) of displacement of [^{3}H]-CP 55,940 (0.5 nM) from hCB$_1$ receptor, at a compound concentration of 10 μM.
[b] Data reported as percent (n = 2) of displacement of [^{3}H]-WIN 55,212-2 (0.8) from hCB$_2$ receptor, at a compound concentration of 10 μM

Table 2. Scoring functions employed for the MOE-Dock pose selection

Compound	S	E_conf	E_place	E_score1
SR144528	-157.3931	1.4011	-19.8080	1.2020
Ia	-135.3052	3.2078	-20.1970	2.1732
Ib	-141.6427	1.4002	-18.1348	2.6171
II	-153.1774	1.6002	-18.9386	2.1852
III	-143.7722	1.0000	-19.9464	-3.1586
4a	-94.5431	1.0045	-16.7433	2.0341
4b	-112.5643	2.0145	-14.6722	1.3451
4c	-108.5467	1.2211	-11.6521	1.1132
4d	-102.9852	1.0011	-10.7833	1.3245
4e	-115.3241	2.6512	-11.6532	1.0000
4f	-103.6571	2.1103	-18.3421	2.1542
4g	-113.6749	1.6721	-17.5623	2.0911
4h	-100.0087	1.0032	-16.5621	1.0032
4i	-98.5431	1.2211	-17.3242	1.0009

S is the final score, corresponding to the latest refinement process (see experimental section).
E_conf represents the energy of the conformer
E_place is the calculated score from the placement stage.
E_score1 corresponds to the first refinement process (see experimental section)

Ligand-based homology modelling of the human CB_2 receptor SR144528 antagonist binding site: a computational approach to explore the 1,5-diaryl pyrazole scaffold

Elena Cichero, Sara Guariento, Giulia Menozzi and Paola Fossa*

Department of Pharmacy, University of Genoa, Viale Benedetto XV,3 - 16132 Genoa, Italy

* Corresponding author: phone: +39-010-3538238; fax: +39-010-3538358; e-mail:fossap@unige.it

Captions to Figure

Figure 1. Chemical structure of the cannabinoid receptor ligands SR141716A and SR144528. The chemical structure of compounds **Ia, Ib**, **II** and **III** and also of one of the in-house pyrazoles (compound **4g**) are also reported.

Figure 2. Schematic representation of the Ligand-based Homology Modelling (LBHM) protocol here applied. The transmembrane domains (TMs) surrounding the standard HM agonist binding site and the LBHM antagonist one are depicted in red and green respectively.

Figure 3. Top-view of the final refined LBHM of the human CB_2 antagonist binding site. The SR144528 pose is also reported, in stick and coloured by atom type (*C* atom: cyan). The transmembrane domains delimiting the putative antagonist binding cavity are coloured in green.

Figure 4. Docking pose of SR144528 (stick, coloured by atom type, C atoms in deep pink) into the human CB_2 receptor binding site. The most important residues are labelled.

Figure 5. Docking pose of **Ia** (stick, coloured by atom type, C atom in light green) into the human CB_2 receptor binding site. The most important residues are labelled

Figure 6. Docking pose of **II** (stick, coloured by atom type, C atom in pink) into the human CB_2 receptor binding site. The most important residues are labelled

Figure 7. Docking pose of **III** (stick, coloured by atom type, C atom in cyan) into the human CB_2 receptor binding site. The most important residues are labelled

Figure 8. Docking pose of SR144528 and of **4g** (stick, coloured by atom type, C atoms in deep pink and in light green, respectively) into the human CB_2 receptor binding site. The most important residues are labelled.

Figure 9. Docking pose of SR144528 and of **4e** (stick, coloured by atom type, C atoms in deep pink and in dark cyan, respectively) into the human CB_2 receptor binding site. The most important residues are labelled.

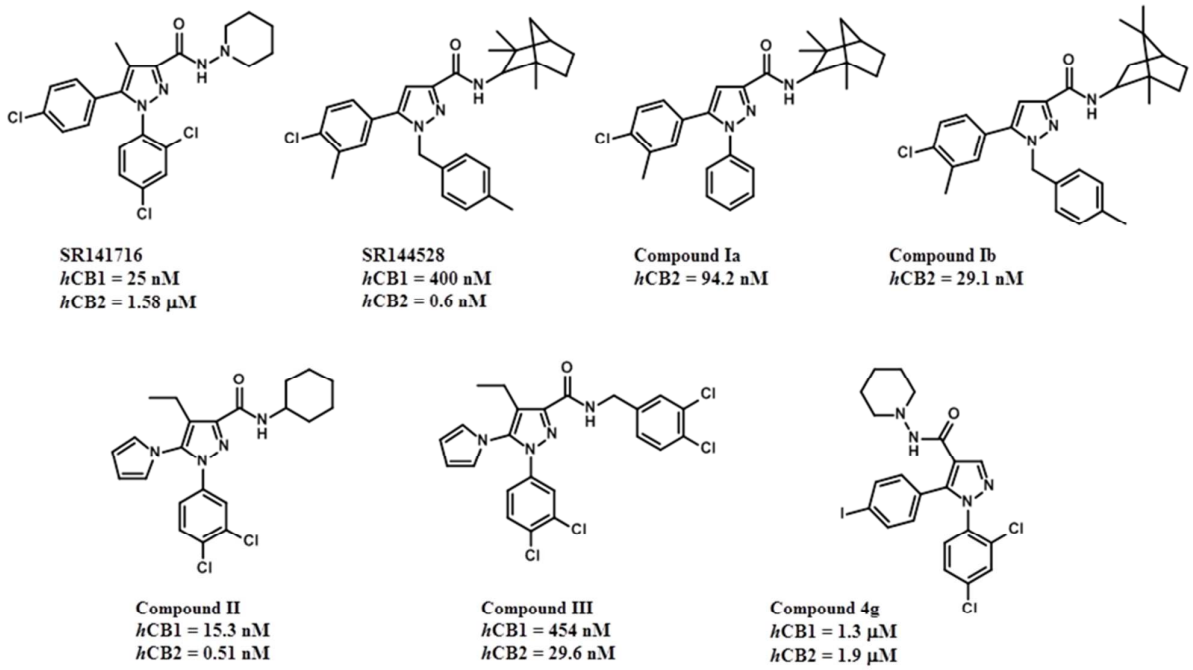
SR141716
hCB1 = 25 nM
hCB2 = 1.58 µM
SR144528
hCB1 = 400 nM
hCB2 = 0.6 nM
Compound Ia
hCB2 = 94.2 nM
Compound Ib
hCB2 = 29.1 nM
Compound II
hCB1 = 15.3 nM
hCB2 = 0.51 nM
Compound III
hCB1 = 454 nM
hCB2 = 29.6 nM
Compound 4g
hCB1 = 1.3 µM
hCB2 = 1.9 µM

Figure 1

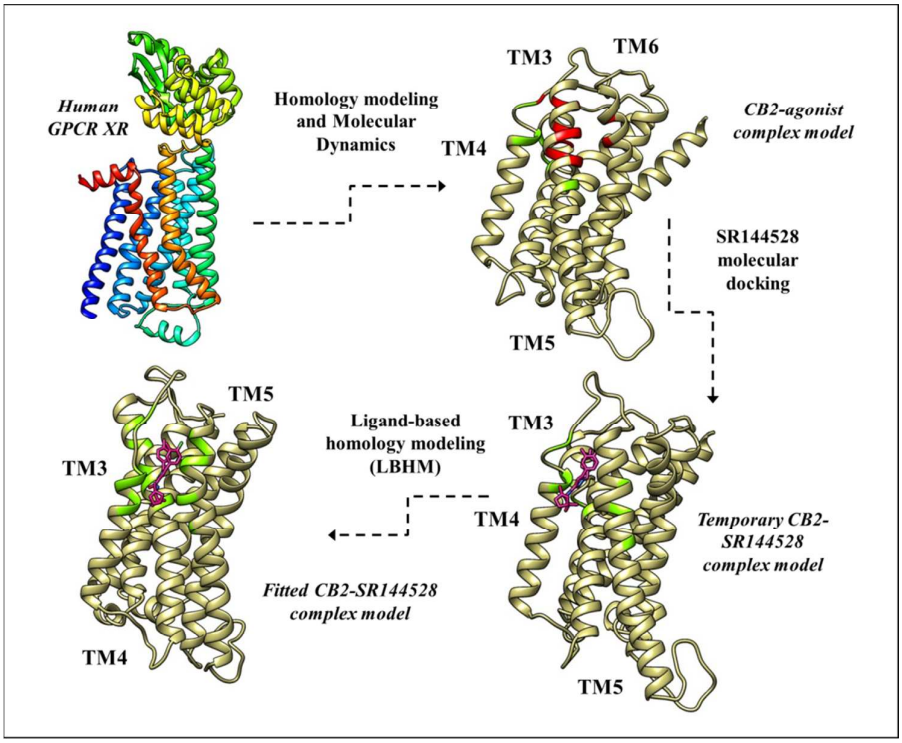
Human
GPCR XR
Homology modeling
and Molecular
Dynamics
TM3
TM6
TM4
CB2-agonist
complex model
SR144528
molecular
docking
TM5
TM5
TM3
Ligand-based
homology modeling
(LBHM)
TM3
TM4
Temporary CB2-
SR144528
complex model
Fitted CB2-SR144528
complex model
TM4
TM5

Figure 2

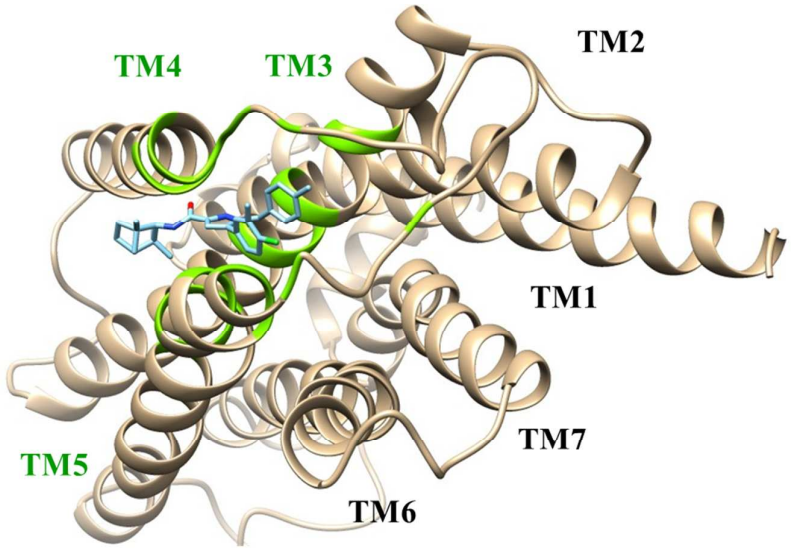

Figure 3

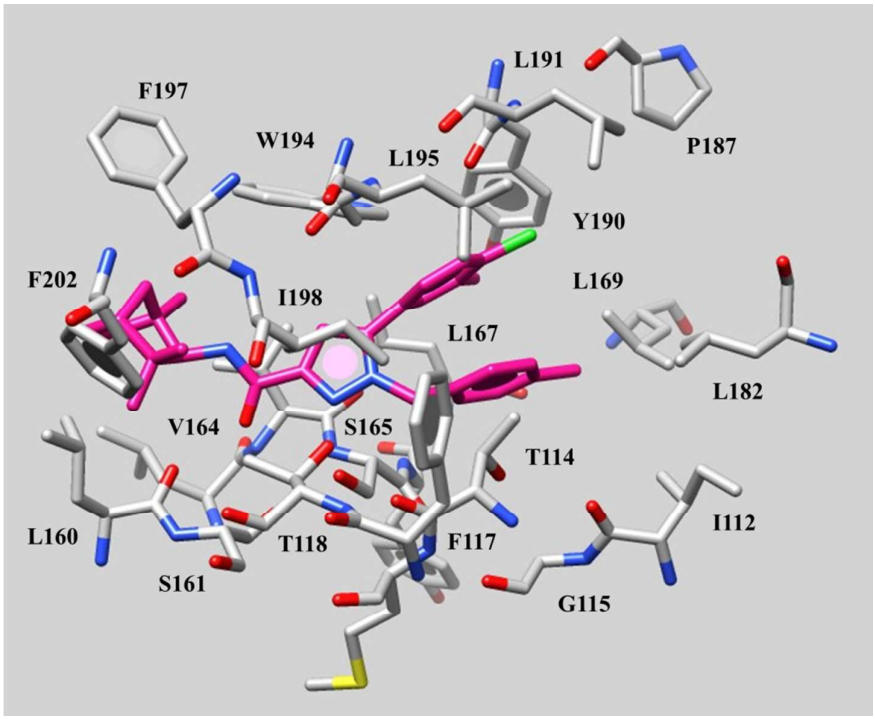
L191
F197
W194
L195
P187
Y190
F202
I198
L169
L167
L182
V164
S165
T114
I112
L160
T118
F117
S161
G115

Figure 4

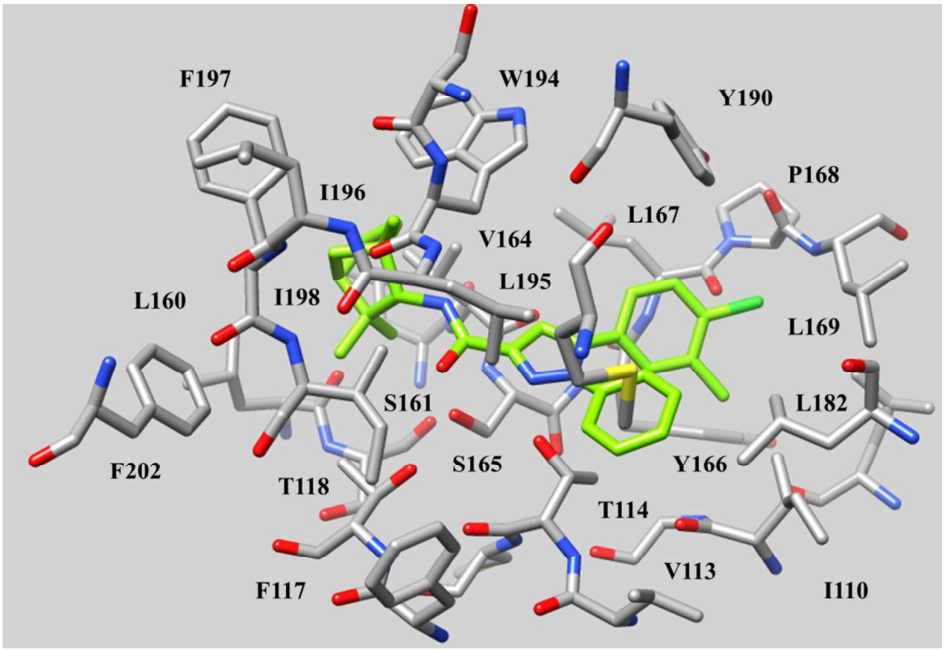
F197
W194
Y190
P168
I196
L167
V164
L195
L160
I198
L169
S161
L182
F202
S165
Y166
T118
T114
V113
F117
I110

Figure 5

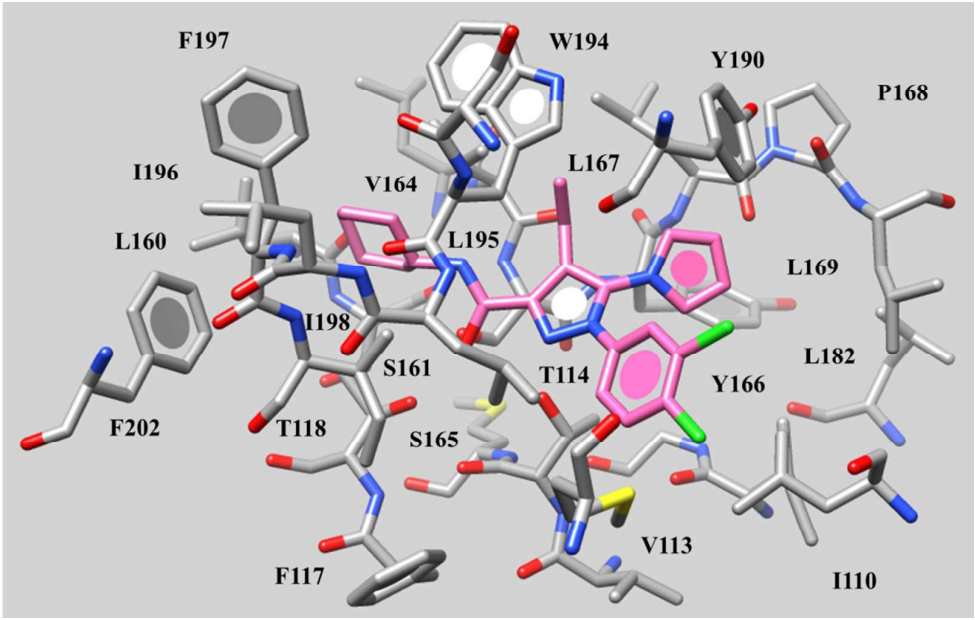
F197
W194
Y190
P168
I196
V164
L167
L160
L195
L169
I198
S161
T114
L182
Y166
F202
T118
S165
V113
F117
I110

Figure 6

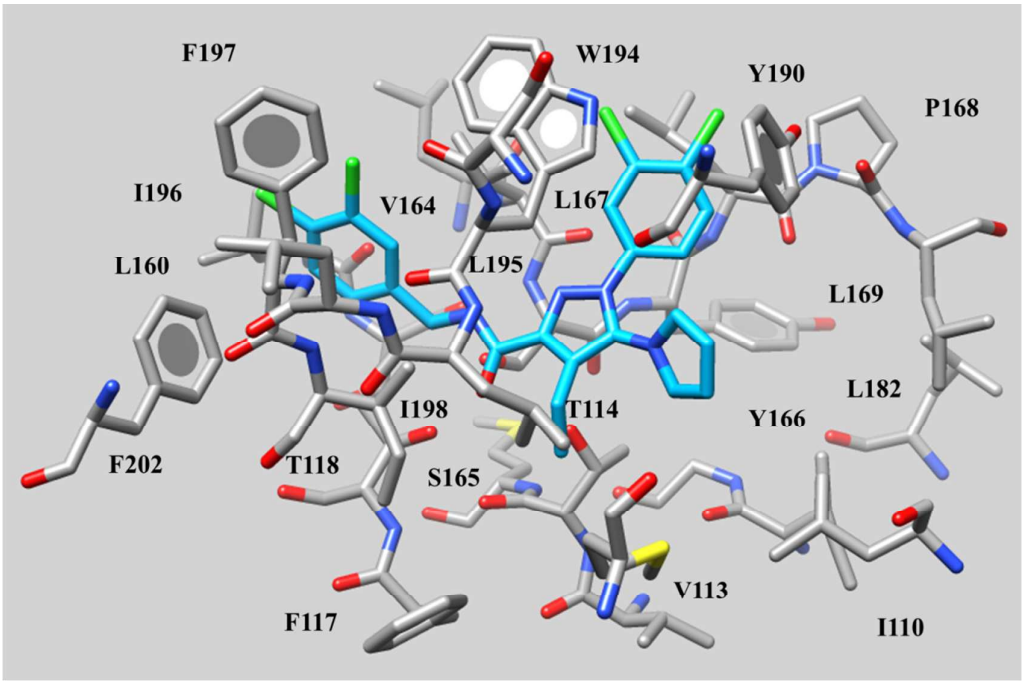
F197
W194
Y190
P168
I196
V164
L167
L160
L195
L169
L182
I198
T114
Y166
F202
T118
S165
V113
F117
I110

Figure 7

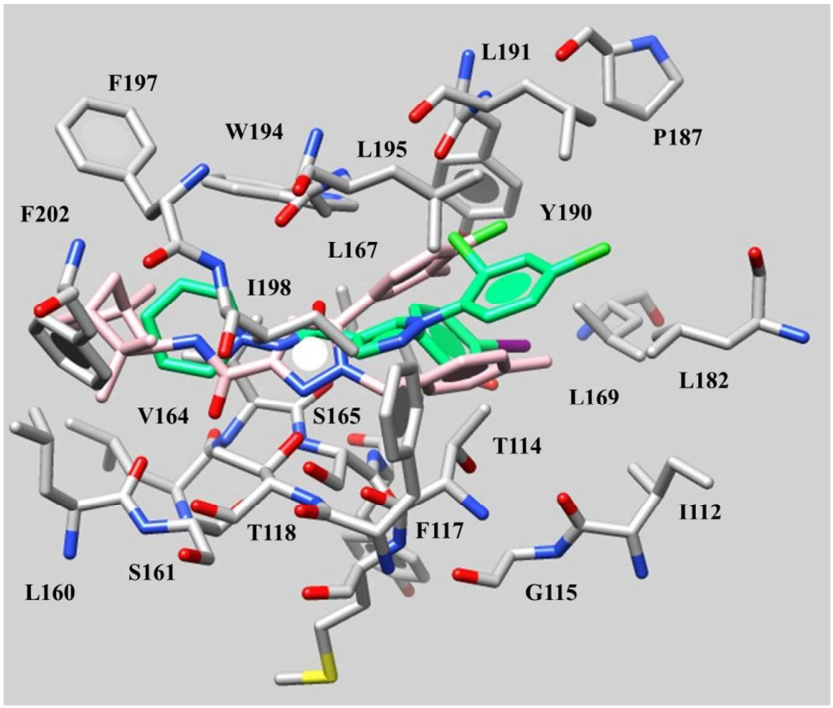
L191
F197
W194
L195
P187
F202
Y190
L167
I198
L182
L169
V164
S165
T114
I112
T118
F117
S161
L160
G115

Figure 8

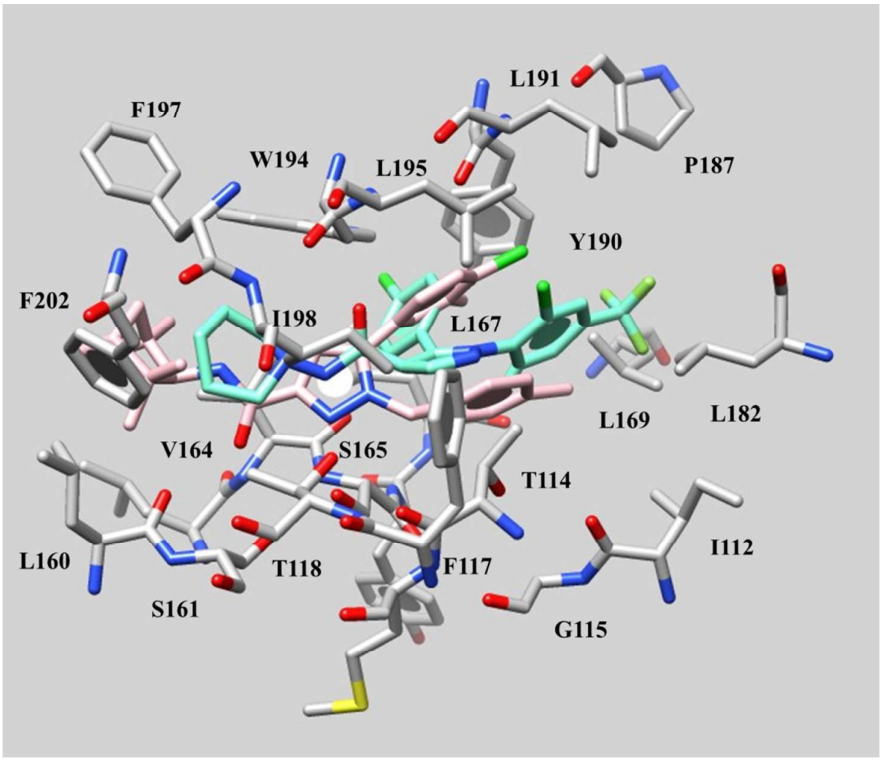
L191
F197
W194
L195
P187
Y190
F202
I198
L167
L169
L182
V164
S165
T114
I112
L160
T118
F117
S161
G115

Figure 9

Ligand-based homology modelling of the human CB_2 receptor SR144528 antagonist binding site: a computational approach to explore the 1,5-diaryl pyrazole scaffold

Elena Cichero, Giulia Menozzi, Sara Guariento and Paola Fossa*

Department of Pharmacy, University of Genoa, Viale Benedetto XV,3 - 16132 Genoa, Italy

*Corresponding author: phone: +39-010-3538238; fax: +39-010-3538358; e-mail:fossap@unige.it

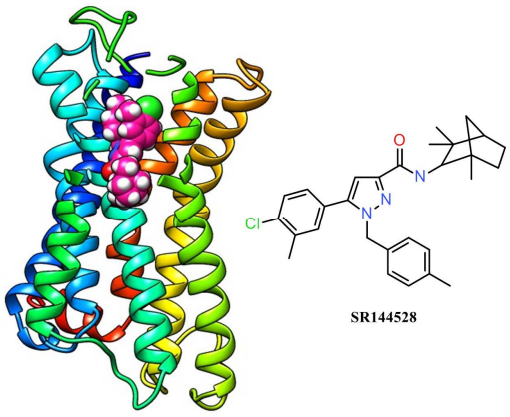

SR144528 docking mode into the LBHM of the human CB_2 receptor antagonist binding site